Evaluation and comparison of hydroxyapatite coatings deposited using both thermal and non-thermal techniques

J. N. Barry[1], B. Twomey[2], A. Cowley[3], L. O'Neill[2], P. J. McNally[3] and D. P. Dowling[1]

[1] School of Mechanical & Materials Engineering, University College Dublin, Belfield, Dublin 4, Ireland

[2] EnBio Ltd., Belfield Innovation Park, University College Dublin, Belfield, Dublin 4, Ireland

[3] School of Electronic Engineering, Dublin City University, Dublin 9, Ireland

Abstract

This paper compares the properties of hydroxyapatite (HA) coatings, obtained using two different deposition technologies on Ti-6Al-4V substrates. The deposition techniques evaluated were: atmospheric plasma spray (APS, thermal treatment) and a novel micro-blasting technique known as CoBlast (non-thermal treatment). The HA coatings were examined with respect to their morphology, crystallinity and adhesion, while the phase concentration of the metallic substrates were also analysed. *In vitro* cell proliferation and cell morphology studies using MG-63 osteoblastic cells were carried out on the HA coated substrates obtained using the two deposition techniques, with untreated titanium grade 5 (Ti-6Al-4V) substrates utilised as a control. XRD analysis of the CoBlast deposited HA coatings demonstrated that it was comprised of the same crystalline HA as the precursor powder. For the APS HA coatings however, additional calcium phosphate phases were observed, and these were attributed to phase changes caused by the high plasma deposition temperatures. The APS treated samples also exhibited evidence of substrate modification, with substrate conversion to a β-rich surface at the HA/substrate interface was observed in the XRD analysis. CoBlast HA coatings, with an average thickness of approx. 2.5 µm, were found to have higher tensile adhesion values (33.6 and 35.7MPa), when compared with the 5 MPa obtained for the approx. 26.9 µm thick APS coatings using a modified tensile adhesion test. This lower adhesion tensile value is most likely due to the increased residual stress generated in the HA coating during thermal plasma processing. The cell response studies on the four surfaces tested indicate that the HA surfaces exhibited higher levels of cell proliferation than the untreated titanium after 5 days, with the CoBlast surfaces displaying statically significant increases in cell proliferation.

1 Introduction

Hydroxyapatite (HA) is a calcium phosphate apatite, and is the main mineral component of bone tissue [1, 2]. HA is also classified as an osteo-conductive and biocompatible material [1, 3], which has led to its extensive use in orthopaedics, dentistry and maxillofacial reconstructions [3-6]. Despite its biological properties, in its bulk form, HA is brittle and has poor tensile strength and low impact resistance [1, 6]. Consequently, in orthopaedics and dentistry, HA is more often applied as a coating to enhance the biological response of metallic implants, while the durability and functionality is provided by the substrate metal [1, 2, 7].

A number of different methods are available for the deposition of HA coatings. Amongst these are: sol-gel [2, 6, 8, 9], ion-beam sputtering [2, 3, 6, 10], electrophoretic deposition [2, 6, 11, 12], high-velocity oxy-fuel spray (HVOF) [6, 13, 14] and Atmospheric plasma spraying (APS) [1-3, 6, 14-17]. Of these, APS is the most widely applied commercially for the coating of medical implants [3, 6, 17]. A number of authors have reported concerns regarding the crystalline phase change of the HA powder and the substrate grain structure during the high temperature APS process [1, 6, 15]. They have highlighted the formation of alternative HA phases, these phases can give rise to HA coatings with higher dissolution rates and reduced long term fixation to bone *in vivo* [1, 18, 19]. It is widely accepted that thermal deposition processes, like APS, result in HA coatings with higher induced residual stresses, and thus, decreased tensile bond strengths [20-22]. Furthermore, reports have shown these types of deposition processes can affect the substrate's properties and reduce the long term performance of an implant [20, 23-26]. The metallic substrate can typically reach temperatures of 400-500°C during the APS process [23, 27]. Reports have indicated that rapid increases and decreases in temperatures can alter the ratio at which the titanium α and β phases are present within a titanium alloy, consequently affecting the mechanical performance of the substrate material [28]. This issue could be amplified when applying such coatings onto small mass implant devices, such as; dental implants or fixation screws/plates [29]. This is due in part, to the lower surface area to volume ratio associated with these devices, and also the inability for these devices to dissipate the heat generated during the deposition process. As a consequence, interest in alternative deposition techniques, which offer retention of the powder's crystallinity as well as minimizing the thermal impact on the substrate material is increasing [30]. There are alternative low temperatures techniques currently available for the deposition of HA coatings, such as electrophoretic depositions and sol-gel [2, 6, 11, 12, 31]. These techniques however, typically require a subsequent high temperature process (or sintering process) to bind the coating both together and to the substrate surface [2, 11, 12, 31]. The issues and limitation regarding this thermal treatment process have been well documented previously, particularly for titanium based substrates [32-34].

This paper reports on a co-incident micro-blasting technique, called CoBlast for the deposition of HA coatings onto titanium grade 5 substrates [35]. Titanium grade 5 is the most frequently used material in load bearing orthopaedic applications, particularly in the area of small mass implants due to its relativity low density (4.5 g/cm^3). In the CoBlast process, HA particles entrained in a compressed air jet are deposited onto metallic substrates, in conjunction

with a coincident jet of abrasive particles [35-37]. The principal advantages of the CoBlast technique are the simple operation, relatively low capital cost of the processing equipment and the low deposition temperature attained during coating deposition. The latter should help to avoid the HA crystalline phase changes and increased substrate temperatures highlighted previously for APS deposited HA coatings [23, 27, 38]. Studies have shown the CoBlast process produces biocompatible HA surfaces which promote lamellar bone formation at the interfacial surface [37]. Hence the CoBlast technique has considerable potential for the modification of small implant surfaces with HA. As CoBlast is a comparatively new deposition technology, the primary objective of this study is to compare the properties of HA coatings deposited using this technique with those from the widely applied APS process. A further objective is to compare the effect of two abrasives powders utilised in the CoBlast depositions (alumina and a sintered apatite known as MCD), on the properties of the deposited HA coatings.

2 Materials and Methods

2.1 Materials and Sample preparation

HA powder with a particle size range of 25-60 µm was purchased from S.A.I. (Science Applications Industries, France). To remove any retained moisture that may hinder powder flow, the HA powder was heated to 150°C for 1.5 hours prior to the deposition experiments. Two abrasive powders were utilised in the CoBlast process to facilitate the evaluation of the abrasive powder's influence on deposited HA properties. These where: MCD (A sintered apatite with a particle size 102 µm) and Al_2O_3 (with mean particle size of 100 µm). These were purchased from Himed (USA) and Comco Incorporated (USA) respectively. Scanning electron micrographs of the powders used in this study are shown in Fig 1.

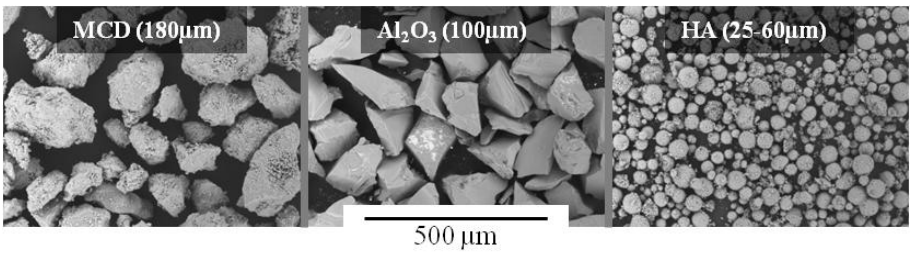

Fig 1 Scanning electron moicrographs of the powders used and their mean particle sizes (scale bar = 500µm)

The studies were carried out on titanium grade 5 alloy (Ti-6Al-4V) substrates, with dimensions 15 x 15 x 1 mm obtained from Lisnabrin Engineering Ltd (Ireland). The substrate thickness of 1 mm was selected in order to facilitate close representation of small mass implant devices, such as dental implants, fixation screws and plates. Similar sample dimensions have been used in previous work with both CoBlast and APS studies [39-43]. The substrates were polished with 1200 grit silicon carbide paper. The polished samples were then ultrasonically cleaned consecutively in methanol and acetone for 5 minutes each to remove any loosely adherent particles.

The APS deposited HA coatings were supplied by a commercial provider of APS coatings, it is important to note however, both the CoBlast and APS deposition experiments were performed using the same HA powder and titanium test coupons. The APS deposited HA coatings were immersed in deionised water and ultrasonically cleaned for 5 minutes, and dried in an oven at 50°C prior to evaluation.

2.2 CoBlast process equipment/parameters

The CoBlast processing chamber (Fig 2) consists of the abrasive and HA jet system mounted in a sealed glove box, above an X-Y slide table. The slide table facilitates motion of the substrates beneath the nozzles. A containment bag encloses the working environment in which the deposition process is conducted. The HA and abrasive powders are delivered to an area on the titanium surface (or 'blast-zone') through the nozzles using two Comco Accuflo powder feeders. A schematic of the CoBlast applicator is also given in Fig 2.

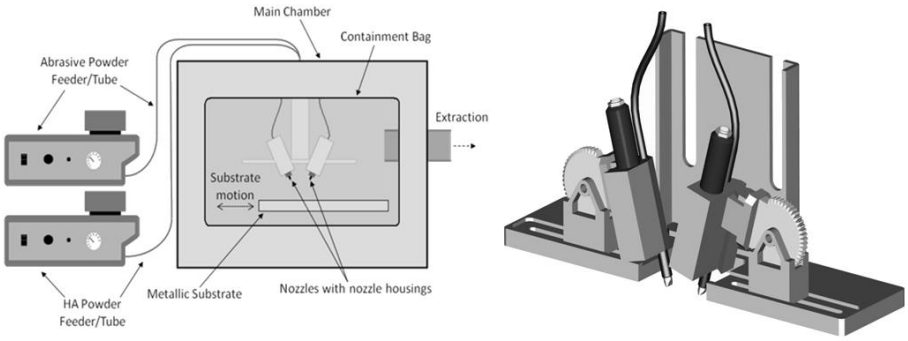

Fig 2 (LEFT) Schematic of the CoBlast deposition equipment, (RIGHT) Dual nozzle CoBlast applicator design

Table 1 details the deposition parameters used in this study. The HA coating surfaces were deposited by passing the polished titanium substrates through the coincident blast-zone, using a 2 mm raster pattern at ≈10 mm/s. Following the CoBlast process, the samples were immersed in deionised water and ultrasonically cleaned for 5 minutes to remove any residual non-adhered HA particles. The samples were then dried in an oven at 50°C.

Table 1 Deposition parameters for the CoBlast coated samples

Material Type	Particle Size (μm)	Angle (°)	Height (mm)	Pressure (PSI)
HA	25-60	80	20	585
MCD/Al_2O_3	102/100	80	20	415

2.3 HA coating and titanium alloy analysis

A TM-1000 Hitachi high-technologies scanning electron microscope (SEM), set in back-scatter mode, was utilised to examine the HA coatings. Surface morphology and cross sectional images were taken at 8 random points on 3 samples of each HA interface examined. Digimizer software (MedCalc Software, Mariakerke, Belgium) was employed on the cross sectional images to facilitate thickness data for the deposited HA layers to be obtained. The

samples were prepared for cross sectional imaging by mounting in polyester resin blocks, cutting transverse sections of the blocks and polishing to a sub-micron finish.

A WYKO NT1100 optical profilometer, operating in vertical scanning interferometry (VSI) mode with a resolution of 3 nm per individual measurement, was utilised to measure the roughness component (R_a: Arithmetic average) of the HA surface. Measurements were taken at a magnitude of x 51.5, over 10 random areas (area dimensions: 120 x 91 μm) on 5 samples of each HA surface. To further facilitate the examination of the metal substrate immediately beneath the coating, the HA layers were etched away by immersion in a 1M HCl solution for 1.5 minutes and samples were then re-examined.

2.4 Chemical and crystallinity analysis

An Energy Dispersive X-ray (EDX) spectroscopy module (Swift-ED, Oxford Instruments Analytical) attached to the Hitachi SEM, operating at an acceleration voltage of 15 kV and a magnitude of x 200, was utilised for semi-quantitative analysis of the HA coatings, and benchmarked against the precursor HA powder. The EDX analysis was carried out over 8 random points on 3 samples of each coating type, using a raster scan to obtain a realistic average of elements present. This technique was also used in conjunction with the HCl etched titanium surfaces to confirm that no calcium or phosphorous was present post acid etching.

X-Ray Diffraction (XRD, Siemens D500 system) was performed to assess coating crystallinity. The HA coatings were analysed over the detector range of 25° to 40° with a resolution of 0.02° and a grab time of 3 seconds. The XRD scans were also carried out on compressed tablets of the HA precursor powder for comparison with the XRD spectra obtained from the CoBlast and APS deposited HA coatings. In addition, XRD using a high resolution Bede D1 system, was performed on the HCl etched substrates over the detector range of 20° to 64°, to examine the substrate crystallography before and after HA deposition. A spectra fitting software called Maud (Materials Analysis Using Diffraction) was utilised to evaluate the XRD spectra obtained from both the HA coatings and the titanium alloyed substrates [44-47]. The MAUD software requires crystallographic information files (CIFs) to fit and quantify each specific material phase within a XRD spectrum. The CIFs utilised in the evaluation of the HA coatings were; TCP (COD: #9005865), HA (COD: #4317043) and TTCP (COD: #9011144), and those in the substrate evaluations were; α – Ti (COD: #9008517), β – Ti (COD: #9008554), TiO2 (COD: #9008976), Rutile (AMCSD: #0011762), Anatase (AMCSD: # 0011765) and Al2O3 (COD: #9007496).

Mechanical Testing

The adhesion of the HA coating to the titanium alloy substrate was determined using a modified ASTM F1147 tensile test. Epoxy coated 2.7mm diameter aluminium studs (Quad Group Inc., USA) were fixed and cured to the HA coatings for 1 hour at 150^{o}C and then left to cool to room temperature. The tensile tests were performed after a preload of 1-2 MPa was reached at a load rate of 0.5 mm/min. The bond strength (Force/Area) was determined by measuring the force required to remove the stud from the surface using an Instron tensile tester. EDX analysis was

carried out on the studs and titanium surface after pull-testing to examine the level of HA removal and to evaluate if failure had occurred at the stud/epoxy interface. The tensile bond test results were calculated based on an average of 5 separate tests. It is important to note that that the substrate thickness at 1 mm used in this pull test study is significantly lower than that specified in the ASTM F1147 standard (0.25" or ≈ 6 mm). The lower thermal mass of the substrate will result in an increased substrate temperature during processing and this will have a direct effect on increasing the residual stress and decreasing the tensile strength of the HA layer [21, 22]. However, the use of a thin substrate sample was chosen as this is representative of the small diameter implants used in many dental and trauma devices.

2.5 In vitro analysis

2.5.1 Cell Culture

MG-63 cells (American Type Culture Collection, Rockville, MD, USA) were cultured in Minimum Essential Medium (MEM) supplemented with 10% foetal calf serum and antibiotic/antimycotic (penicillin G sodium 100 U/ml, streptomycin 100 µg/ml, amphotericin B 0.25 µg/ml, PAA Laboratories GmbH, Austria) in 75cm^3 Nunc tissue culture flasks. Cells were maintained in a humidified atmosphere with 5% CO_2 at 37°C and were sub-cultured when they reached confluence using 0.25%-Trypsin EDTA to provide adequate numbers of cells for the various *in vitro* culture studies undertaken here.

2.5.2 Cell Proliferation

The relative rates of cell proliferation on the different sample types were gauged after 24 hours and 5 days culture. MG-63 cells were seeded on the sample surfaces at a cell density of 1x10^5 cells/cm^2 and incubated as described previously. A commercial MTT assay kit (Sigma-Aldrich, UK) was used to perform the analysis. The MTT reagent is a soluble tetrazolium salt which is yellow in solution. In culture, the dissolved MTT is converted by active mitochondrial dehydrogenases into insoluble, purple formazan crystals. These crystals can then be solubilised and read colorimetrically where the measured absorbance is directly proportional to the number of metabolically active cells. The MTT assay reagent was prepared as a 5 mg/ml stock solution in PBS, sterilized by Millipore filtration, and stored in the dark. At the appropriate time-points, MTT stock solution (10% of total volume) was added to each well containing the samples. After 3 hrs incubation at 37°C in 5% CO_2, the reagent was aspirated, MTT Solvent (Sigma-Aldrich, UK) was added to dissolve the formazan crystals. The optical density of the formazan solutions was read by spectrophotometry on an ELISA plate reader (Tecan Sunrise, Tecan Austria) at 570 nm with the background absorbance value measured at 650 nm. The absorbance values recorded were determined to be proportional to the number of cells attached to the membrane surface in each case.

2.5.3 Cell Morphology

MG-63 cells were seeded onto the various samples at a cell density of 5 x10^5 cells/cm^2 in 6-well plates and were incubated for 24 hours at 37°C in 5% CO2. After 24 hours the samples were gently rinsed with PBS to remove any unattached cells and fixed in a modified Karnovsky's Fixative (2% paraformaldehyde/ 2% glutaraldehyde in PBS) for 1 hour. The samples were then rinsed again in PBS and post-fixed in 1% osmium tetroxide. After again rinsing with PBS (x3), the specimens were dehydrated in an alcohol series (20%, 30%, 50%, 70%, 80%, 90%, 95% ethanol for 15 mins each, and then 3 times in 100% ethanol for 15 minutes). After post fixation, the samples were chemically dried in ethanol:hexamethyldisilizane (HMDS) (1:1) for 30 mins, and 100% HMDS for 1 hour. The samples were then left to air dry overnight. A 50 nm layer of gold-palladium was deposited onto the substrates using a Polaron E5000 SEM Sputter Coating Unit to reduce surface charging effects. The sputtering conditions used a set voltage of 1.4 kV, with a plasma current of 18 mA (argon gas), a deposition time of 2 minutes at a vacuum pressure of 0.05 Torr. SEM images of the cells on each of the surfaces were captured as described above.

3 Results and Discussion

3.1 Thermal analysis of CoBlast depositions

Fig 3 shows a thermal image of the CoBlast deposition process, where the blast-zone, and its pursuing track, are distinguished by the different shades (or gradients of temperature). The thermal studies were performed on the same Ti-6Al-4V substrates as used in the deposition studies. Typically the maximum temperature achieved in the blast-zone was 35°C, however, in some instances the CoBlast processing temperature would increase up to a maximum of 47°C. This increase in processing temperature was particularly evident when the abrasive jet made contact with a sharp edge of a substrate being coated. This processing temperature nevertheless is considerably lower than the particle temperature (>1000°C) and substrate temperature (400-500°C) reported for the APS technique [1, 6, 15, 23, 27]. The CoBlast technique's lower processing temperature should therefore avoid the HA crystalline phase changes that have been highlighted previously for APS deposited HA coatings [23, 27, 38], this will be further examined in this paper using XRD analysis.

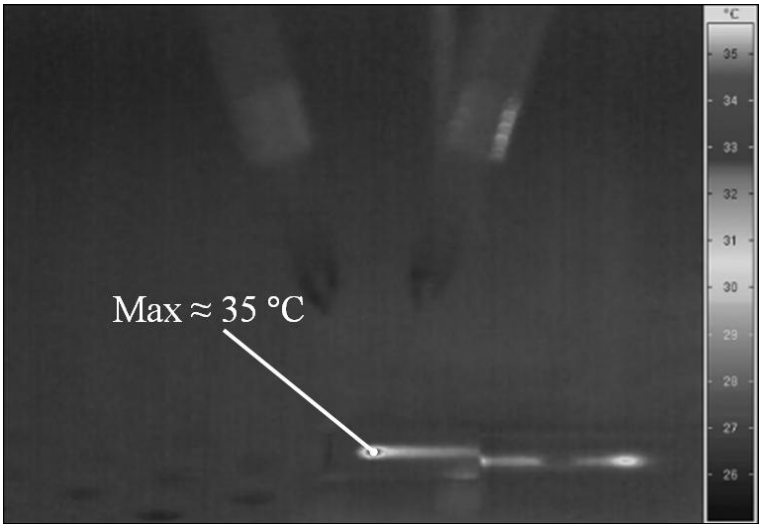

Fig 3 Thermal analysis image of the CoBlast process during HA coating deposition, note the highest temperature observed during the CoBlast deposition studies was ≈ 47°C

3.2 HA interface and titanium substrate analysis

This section details the results of the evaluated CoBlast and APS HA coatings on the Titanium alloy substrates. This analysis includes an investigation of coating morphology and adhesion, cross-sectional examination and phase/compositional analysis. For ease of reference, from this point on the CoBlast deposited samples will be labelled according to the abrasive utilised in their processing. The respective sample names MCD and Alumina are given in Table 2.

Table 2 Referred names for the CoBlast deposition samples produced using the two abrasive powders with mean particle sizes as shown

Abrasive used:	MCD (102)	Al_2O_3 (100)
Sample's name:	MCD	Alumina

3.2.1 HA interface and substrate Morphology

Fig 4 displays the typical morphology and line profile information, obtained using SEM and optical profilometry respectively, for the CoBlast and APS deposited HA coatings. The SEM micrographs showed that the two CoBlast deposited HA coatings exhibit similar morphologies independent of abrasive type. This conclusion is supported by the line profile data obtained for each of the CoBlast HA surfaces (Fig 4B). The APS deposited coating in contrast exhibits a much rougher surface morphology. Cracking was observed on the APS HA coating surface (arrows in Fig 4A). Higher magnification SEM images indicate that the APS deposited HA coating have a glassy appearance, which would suggest that significant melting of the HA powder had occurred during deposition [1]. This glassy appearance was absent from the CoBlast deposited coatings.

The line profiles data in Fig 4B demonstrated that the CoBlast HA surfaces have relatively smooth morphologies compared with the APS deposited coatings. The corresponding roughness measurements are given in Fig 5. It was also noted for the CoBlast process, a change in abrasive type from MCD to Al_2O_3, resulted in an increase in the average R_a values for the HA coatings from 0.84 to 1.31 µm ($P < 0.001$), which may be attributed to the increased abrasion provided by the harder and more angular alumina abrasive (Fig 1).

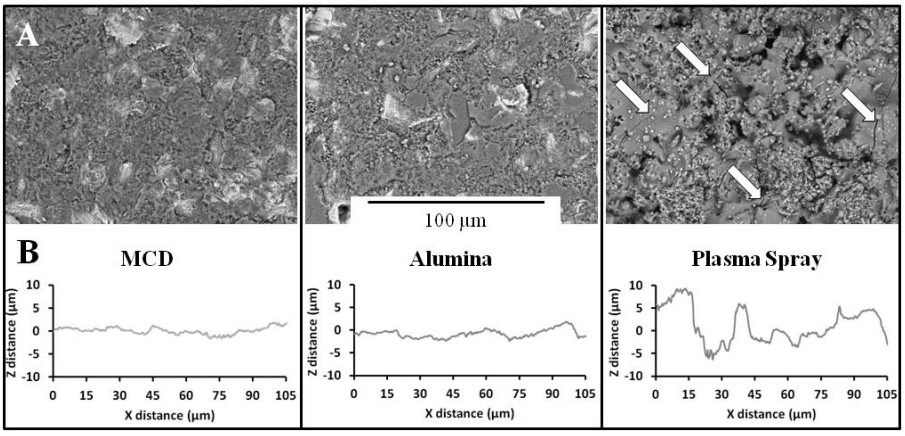

Fig 4 A) SEM surface morphology images, the arrows highlight cracking in the APS coating (scale bar for all images = 100µm), B) Typical line profiles obtained from each of the HA interfaces

The variation in surface finish obtained with the CoBlast and the APS deposited coatings can be explained by the individual processes. Prior to APS processing, the substrate is subjected to a grit-blasting process using an alumina grit with mean particle size >350 µm. This process is used to increase the available surface area onto which the HA coating can bond, by significantly increasing the substrates roughness.

During the APS process, HA particles are rapidly heated within a plasma flame, forming molten or partially molten particles which are proportional to the precursor particle size [1]. These are then projected toward the substrate surface and impact the substrate forming splats, which rapidly cool to form mounds. It is thought that the grit-blasting process combined with the solidification of the semi-molten particles is what yields this increased roughness with the APS deposited HA coatings, when compared with the CoBlast treated samples [1, 48]. The roughness results and line profiles would support this conclusion; with the APS HA coatings exhibiting profiles that are on the scale of the original powder particles (25-60 µm), cross sectional data (Fig 6) would also support this suggestion with the thickness of the APS deposited coatings being in the order of the precursor particle size. In the case of the CoBlast process, HA is integrated into the surface by the removal of the metal substrate's oxide layer via the abrasive jet, while the coincident jet of HA particles shatter upon impacting the freshly exposed metal surface, which consequently spreads HA across the activated surface. The particle shattering is apparent in the SEM images, where very few large grains are visibly within the coating. The line scans of the HA surfaces also show the absence of peaks on the scale of the precursor powder. O'Hare et. al. suggests this method of HA deposition results in both chemical and mechanical bonding between the substrate and HA [37].

Fig 5 provides roughness (R_a) data for the HA surfaces and titanium substrates after the HA was removed in dilute HCl. It is interesting to note that the deposited HA layer significantly increases ($P < 0.025$) the surface roughness in the case of the alumina abrasive CoBlast HA samples, while there is a decrease in the case of the APS HA coatings.

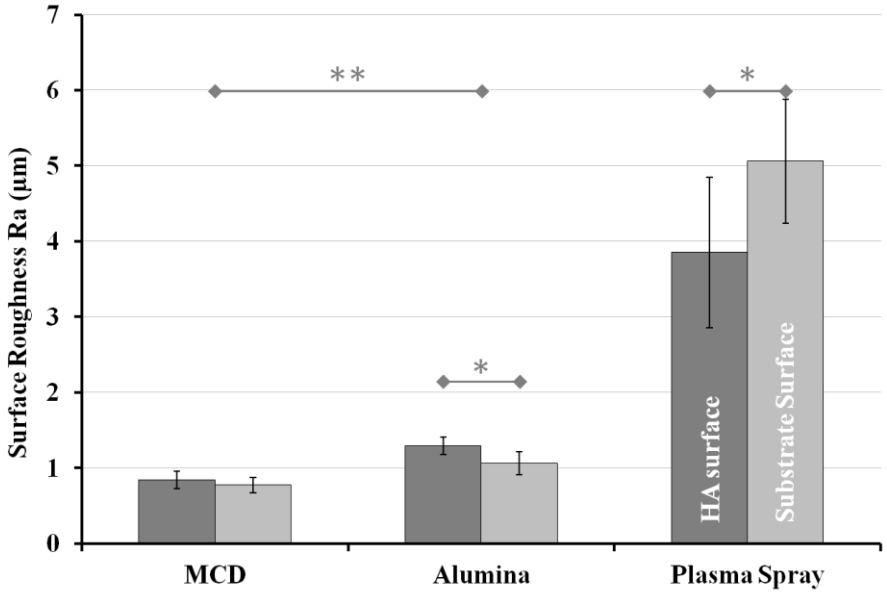

Fig 5 Surface roughness (R_a) obtained for the CoBlast (MCD, Alumina abrasive) and the APS deposited HA coatings. In addition data on the substrate metal roughness after removal of the HA coating is provided also. (* $P < 0.025$, ** $P < 0.001$)

3.2.2 HA interface and substrate cross sections

Fig 6 displays examples of cross sectional images obtained for the two CoBlast and APS deposited HA coatings. The CoBlast HA coatings were found to be of similar thickness, ranging from 2.2 ± 1.1 µm to 2.8 ± 1.7 µm for the MCD and Alumina deposited coatings respectively. Their cross-section morphologies show a dense HA structure and visually exhibit low levels of porosity, with intimate contact at the titanium-HA interface observed. SEM imaging of the CoBlast deposited HA, indicated some differences in the appearance of the titanium alloy beneath the coating layer with the abrasive media. The alumina deposited HA surfaces exhibited more angular features at their titanium-HA interface, when compared to MCD abraded HA surfaces. This observation is supported by the R_a results obtained after acid removal of the HA layer as shown in Fig 5. A possible explanation for this variation in the roughness for the two CoBlast HA surfaces is that MCD is a softer particle, and more rounded than the Al_2O_3 particles as illustrated in Fig 1. It is important to note the limitation CoBlast technique with regards to HA coating thickness, which is in the region of 2 to 3 µm. This is the approximate HA layer thickness deposited in a single pass of the CoBlast jets. During additional passes the abrasive media removes some of the previously deposited layer of HA and also deposits more HA. The overall HA layer thickness however does not significantly increase.

The APS HA coatings with average thickness of 26.9 µm are significantly thicker than the ≈ 2.5 µm obtained using the CoBlast technique. The cross sectional image shows the presence of cracks, which appear to penetrate deep into the APS HA coating (arrows in Fig 6). Similar morphologies and cracking of APS deposited HA coatings have previously been reported [16, 26, 49]. The formation of these cracks has been attributed to the rapid and uncontrolled cooling of the thick HA coatings [1, 16, 26, 49]. The absence of these features in the CoBlast deposited HA surfaces are most likely due to the significantly decreased deposition temperature (<47°C) and lower HA layer thickness. It is suggested that the cracks could lead to weakening of the APS HA coating and/or unexpectedly high dissolution rates, due to the increase surface area offered from within the HA coating. As highlighted previously, HA dissolution at the titanium interface could possibly result in the splintering and delamination of large sections of the HA coating [18]. The fragmentation of APS HA coatings by this mechanism has been reported after fatigue tests under both dry and wet conditions [26, 50]. A further factor that can accelerate HA coating dissolution is the presence of more soluble CaP phases, when compared to crystalline HA (i.e. α –TCP, β –TCP and TTCP), which are typically produced during the APS process [1, 6, 15]. Additionally, Al_2O_3 particles were observed beneath the APS deposited HA coatings in some cross sectional images. These particles are visible at the base of the coating in Fig 6, between the substrate metal interface and HA coating. Dissolution or removal of the APS deposited HA coating could lead to the release of these particles.

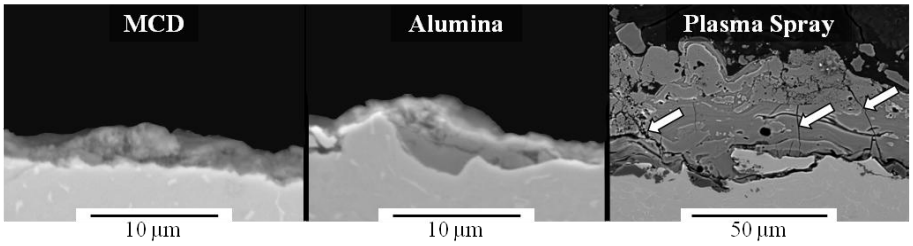

Fig 6 SEM cross sectional images of the HA / titanium alloy interfaces obtained using the CoBlast and APS processes, the arrows signify cracks in the APS HA coating (Scale bars: CoBlast = 10µm, APS = 50µm).

3.2.3 Compositional analysis

EDX analysis was used to examine the weight percent (Wt.%) ratio of the Ca and P elements within the deposited HA coatings and precursor HA powder, the results of which are given in Fig 7. This study found the Ca/P (Wt.%) ratios of the MCD and alumina CoBlast deposited coatings to be 2.3 and 2.5 respectively, which compared well with that of the precursor HA powder (2.4) with no statistically significant variation. Conversely, a statistically significant difference was observed between for the APS HA coatings and the precursor HA powder. This could be due to changes in chemical composition arising from the thermal nature of the APS process [1]. While the HA particles are in their molten state some phosphorus may be lost from the powder, resulting in enhanced levels of Ca. This change could be associated the formation and inclusion of additional calcium phosphate phases (calcium enriched) in the APS HA coatings [51]. XRD crystallinity studies were used to investigate this further.

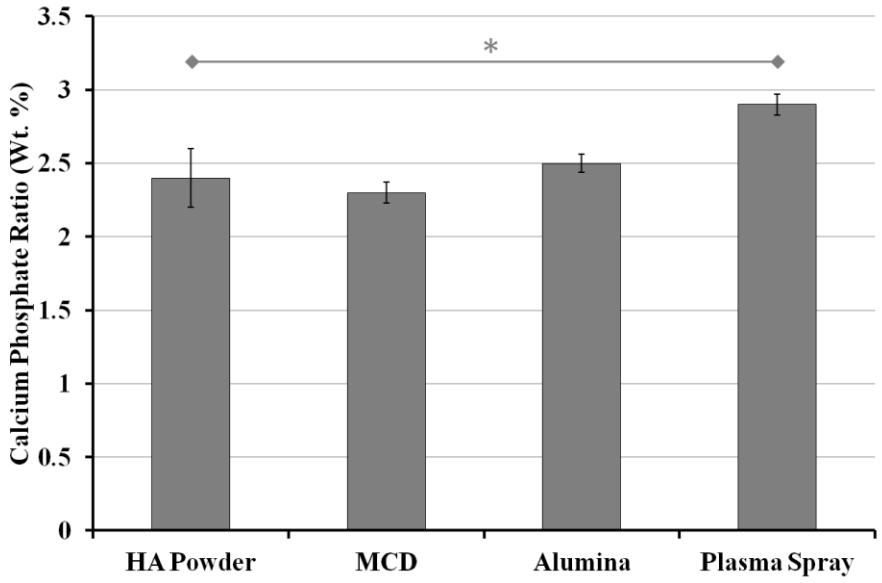

Fig 7 The Ca/P molecular weight ratios of the CoBlast and APS deposited HA coatings obtained by EDX (* P < 0.001)

XRD spectra for the coatings and HA powder are given in Fig 8. For clarity, only the spectrum for the MCD sample is displayed, as almost identical spectra were observed with the alumina samples. Fig 8 shows the CoBlast HA coating has a crystalline structure similar to that of the precursor HA powder. This demonstrates that the low temperature deposition process allows retention of the crystallinity of the precursor HA powder and is in good agreement with the EDX results. The APS HA coatings also exhibit similar peaks to the precursor HA powder. Maud analysis however estimates up to 11 % of the HA material at the coating surface has been converted to different phases (i.e. α – TCP, β – TCP and TTCP). Significantly, the amorphous halo (or glassy HA, indicated in Fig 8), demonstrates further deviation from crystalline HA during deposition [52-54]. The amorphous content in the coating was however not quantifiable using the MAUD software due to inherent limitation in the software. The presence of the Ca-rich phases, TTCP and amorphous HA, within the APS HA coating would account for the relative increase in Ca/P ratio observed in the EDX data. Furthermore, α – TCP, β – TCP, TTCP and amorphous HA are known for their increased solubility relative to crystalline HA. Although the increased solubility of the APS deposited HA coatings may allow for rapid osseointegration compared with the pure HA surfaces, it is however generally associated with the formation of fibrous bone [1] rather than stable, lamellar bone observed previously for CoBlast surfaces [37]. The XRD peak broadening displayed in each of the HA coating spectra has been suggested by Prevéy to be due to the presence of nanocrystalline HA [55].

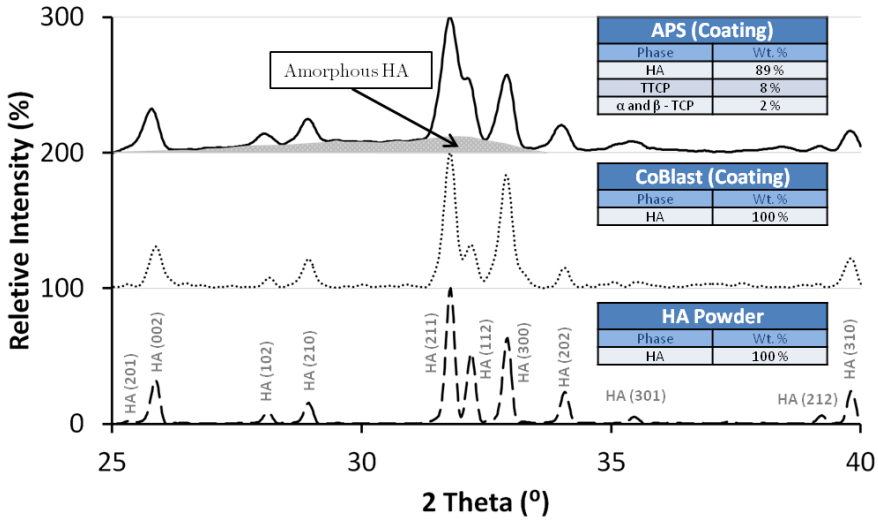

Fig 8 XRD spectra of the APS and CoBlast (MCD) deposited HA coatings, and compared with the scan obtained for the precursor HA powder (Maud values calculated with amorphous phase removed)

The XRD spectra for the titanium alloy substrates after acid removal of the HA layer are shown in Fig 9. The MAUD software was further utilised to examine the substrate XRD spectra, and specifically monitored for α and β phases of the metal titanium as the Ti-6Al-4V is defined as an α-β phase titanium alloy [56]. It is clear from the XRD spectra both the CoBlast and titanium (untreated) substrates are very similar in crystallinity, due to the mirrored relative peak intensities and peak positions. This indicates no thermal changes are induced in the substrate during CoBlast processing. Conversely, the substrates treated using the APS process showed significant deviations from the untreated substrate spectrum. It was observed that the relative peak intensity reduced at the positions 40.5, 53 and 63.5°, while previously undetected peaks appeared at positions 25.7, 43.5 and 52.5°. MAUD analysis indicated that these additional phases were due to the incorporation of alumina particles in the substrate, as shown in Fig 9. No evidence of features due to HA, α – TCP, β – TCP, TTCP or other calcium phases were detected. The MAUD analysis determined that the reduced peak intensities seen at 40.5, 53 and 63.5° reflected a reduction in α phase titanium allowing an increase in the presence of β phase. The phase change seen in the APS treated substrates have previously been reported to occur at high temperatures, and have been suggested to significantly alter the mechanical performance of titanium metal alloys [28] and may contribute to a reduction in fatigue properties [24, 26].

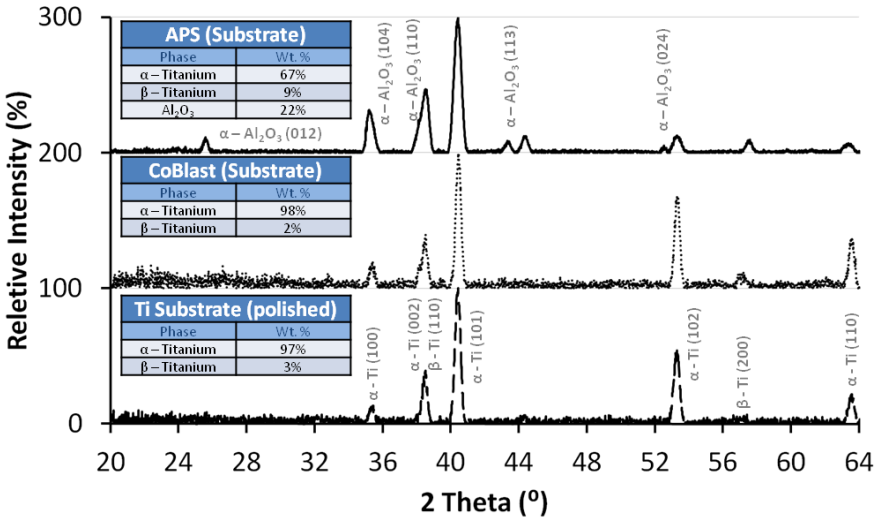

Fig 9 XRD spectra of the titanium substrates (after the removal of the HA coatings) compared with that of the untreated metal. MAUD analysis results for each spectrum are also presented in the tables associated with each of the diffraction patterns (Note that trace levels of Rutile of <0.1% were also detected).

The SEM images (Fig 6) and XRD (Fig 9) demonstrated the incorporation of Al_2O_3 particles at the metal alloy interface in the APS treated samples. This lead to further SEM-EDX investigation of the metal substrates after the acid removal of APS deposited HA coatings. Fig 10 shows the results of this investigation, where large areas of Al_2O_3 (dark grey areas), were observed across the surface of the APS treated substrates, and EDX analysis confirmed the presence of aluminium in the interface. The presence of Al_2O_3 in the APS treated substrates is thought to be from residual particulates left from the grit-blasting process, which is used to increase the metal alloys surface area. This treatment is used prior to the APS process in order to enhance the adhesion of the HA coating and the residual presence of Al_2O_3 particles has been highlighted previously [1, 57].

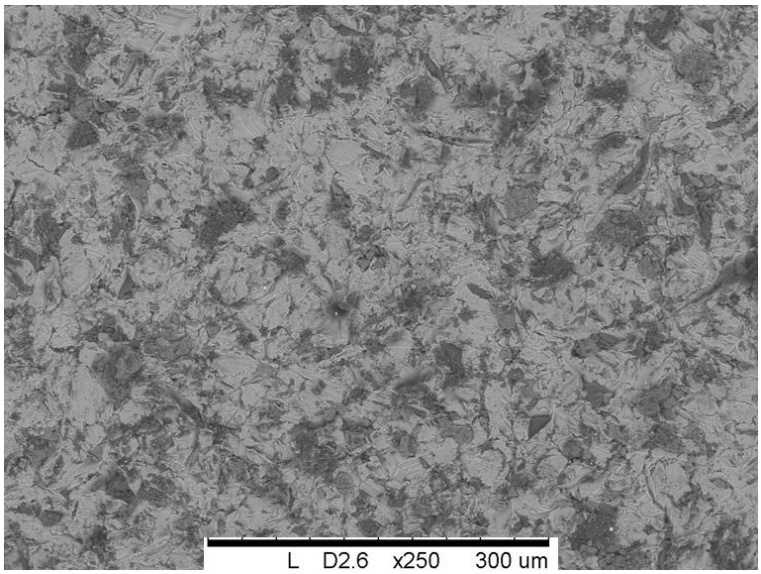

Fig 10 Low magnification SEM micrograph of APSed substrate surface, the light grey is the titanium substrate and the dark grey areas are associated with alumina particles embedded in the coating

In the case of the CoBlast coatings deposited in conjunction with the Al_2O_3 abrasives, there was evidence of isolated shards of Al_2O_3 particles embedded in the substrate surface after removal of the HA layer. The XRD spectra of the CoBlast treated substrates however, did not reflect the presence of these Al_2O_3 particles. It is not known whether there is a similar inclusion of MCD abrasive during the CoBlast process but it is expected to be less of an issue as sintered apatites are readily absorbed and less likely to cause third body wear in articulating surfaces.

3.3 Mechanical Testing

The adhesion of the HA coatings to the Ti-6Al-4V alloy was evaluated using a tensile (pull) test technique. The use of small pull-studs (2.7 mm in diameter: contact area ≈ 5.725 mm^2) enabled the direct testing of the 15 x 15 mm coated coupons rather than using the standard 1 inch coupons specified in ASTM F1147. It is expected that the small pin size and decreased volume of epoxy should facilitate more topological bonding and limit epoxy seepage between cracks and open porosity. The bond strength (force/area) was determined by measuring the average pull-off force required to remove the epoxy bonded stud from the coated surface of 6 samples. Fig 11 displays APS and CoBlast samples after mechanical testing and the results are presented in Fig 12.

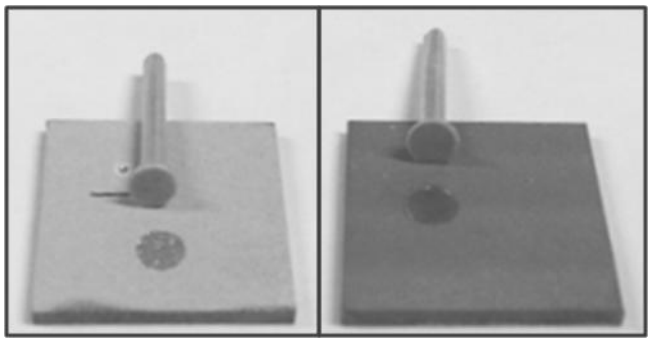

Fig 11 Test pins on the APS (left) and CoBlast (right) HA coated samples after mechanical testing.

A 6% reduction in bond strength was observed between the use of alumina and MCD abrasive for the CoBlast coating deposition. The higher bond strength for the alumina abrasive is likely to be associated with the increased surface abrasion caused by Al_2O_3 particles during deposition. This could result in higher levels of mechanical interlocking at the titanium-HA interface. This conclusion is supported by the higher surface roughness observed on the alumina samples. By comparison however, the APS deposited HA coatings exhibit an 85% reduction in bond strength compared with that obtained for the CoBlast deposited coatings. The significant difference in bond strength between the CoBlast and APS deposited HA coatings may be due to a number of reasons. Firstly the cracking observed in the thicker APS deposited coating may significantly weaken adhesion. Another factor could be that, while the CoBlast HA coatings have reduced potential for mechanical interlocking (lower roughness), the removal of the surface oxide layer during deposition and the subsequent interaction with the HA particles could produces a chemical bond between the HA and the metal substrate as indicated previously [37, 58, 59]. In order to demonstrate

that titanium-HA interface debonding had occurred (adhesive rather than cohesive failure), EDX analysis was carried out on the pull-studs after testing. Significant levels of both Ca and P were observed on the epoxy surface of the pin, while an equivalent drop in Ca and P was observed in the region where the pull test was carried out. From this study it was concluded that the HA layer was predominantly removed via adhesive failure (rather than cohesive failure) from both the CoBlast and APS deposited HA coatings on the titanium surfaces. Only trace levels of Ca and P were observed on these two titanium alloy surfaces after coating removal indicating low levels of cohesive interface failure.

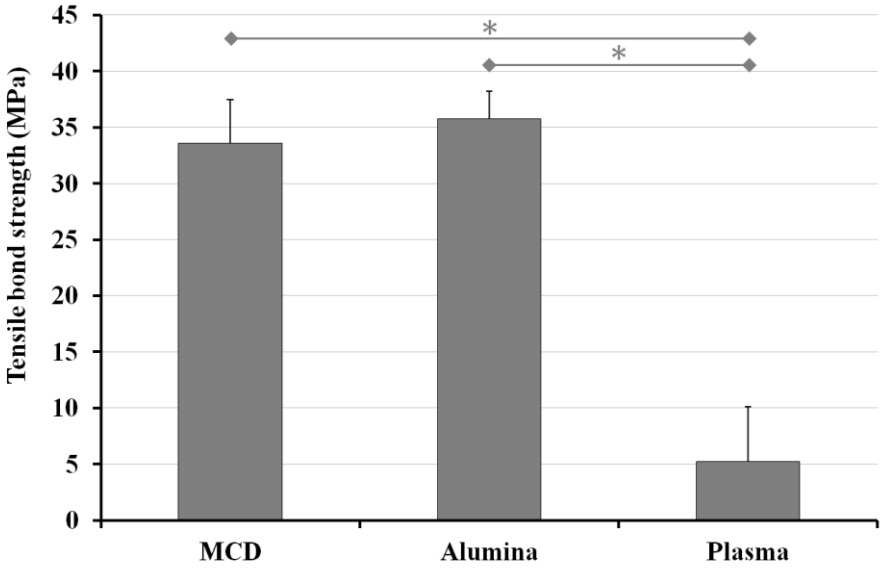

Fig 12 Tensile bond strength measurements obtained for the MCD, alumina and APS deposited HA coatings (* P < 0.001)

3.4 In vitro analysis

MG-63 osteoblastic cell proliferation studies were carried out on the CoBlast and APS HA coatings, with bare Ti-6Al-4V substrates utilised as a control. The results are presented in Fig 13. An unpaired t-test was carried out to determine whether the difference in cell attachment between the surfaces was statistically significant. After 24 hours incubation, there was no discernible difference between the various surfaces, with all four sample sets displaying effective cell attachment. However, after 5 days of incubation there was notably increased cell proliferation observed on the CoBlast surfaces, which were found to significantly outperform the titanium control ($P < 0.025$). The CoBlast samples also showed higher levels of cell proliferation compared with the plasma HA samples at this time point, although this difference was not statistically significant.

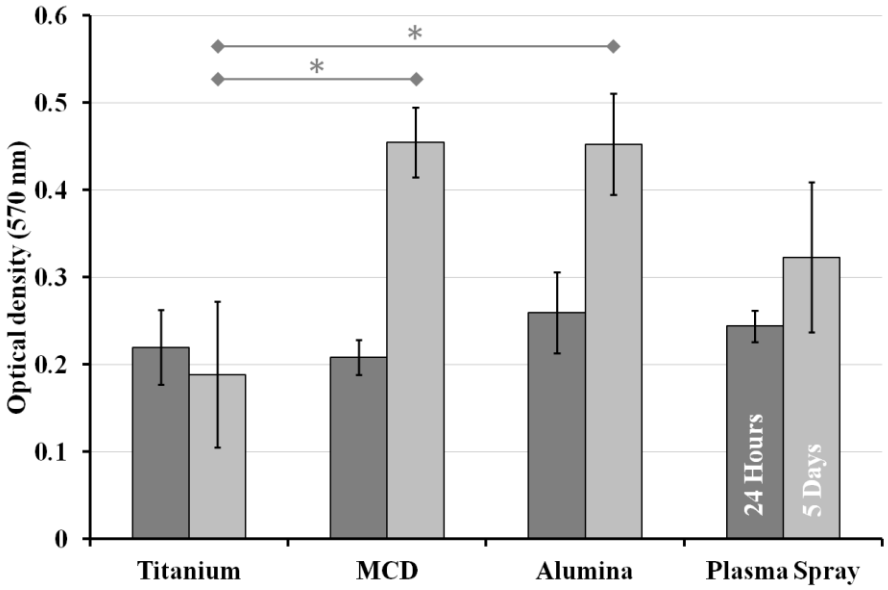

Fig 13 MTT cell proliferation on titanium, CoBlast (MCD and Alumina abrasive) and APS deposited HA. There was a significant increase in cell proliferation on the CoBlast deposited HA coatings (* $P < 0.025$) in comparison to the control surface after 24 hours and 5 days

The morphology of the MG-63 cells on each HA coating was investigated using SEM imaging and typical results are presented in Fig 14. Cells attached well to these surfaces and they displayed a fibroblastic morphology synonymous with that of this cell line, particularly on the titanium control surface. On the CoBlast surfaces extracellular processes such as lamllopodia and filopodia can be seen extending from the main body of the cells onto the surface. The cell morphology was polygonal in appearance, signifying strong cell adhesion to the surface. On the plasma samples, cells appeared to preferentially reside in the pits of the surface. The same observation was noted on the CoBlast surfaces. One possible suggestion for this occurrence is that cells are exposed to a greater surface area and subsequently more focal adhesions between the cell and the surface could be achieved. There was also a significant amount of filopodia present on the surface of the cells on plasma samples, but not as many were identified on this surface type compared to the cells on the CoBlast treated surfaces.

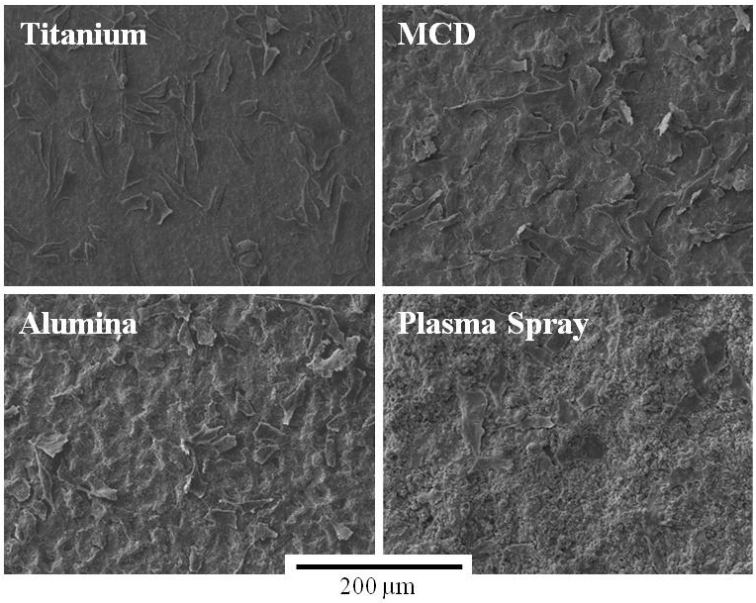

Fig 14 MG-63 cell growth on untreated titanium (top left), CoBlast MCD (top right) and Alumina (bottom left) HA and APS HA (bottom right) after 24 hours culture (Scale bar in each image = 200µm)

After 24 hours, *In vitro* evaluation of the coatings clearly shows that all CoBlast HA and APS HA coatings outperform the titanium substrate with respect to the level of cell proliferation. The MTT assay also showed significant proliferation of cells on the apatite surfaces after five days of incubation. The CoBlast samples were found to have significantly higher levels of cell proliferation (P <0.025) when compared to the control surface. The CoBlast surface also appears to have more cell proliferation than the plasma coating, despite the higher roughness of the plasma HA surface, which is known to enhance osteoblast proliferation. The presence non-uniform surface features (unstable amorphous phases, additional crystal structures) on the APS deposited coatings might be limiting cell proliferation over the entire surface over longer time points and this is reflected in the 5 day MTT assay.

4 Conclusions

The CoBlast and APS techniques were used to deposit HA coatings onto Ti-6Al-4V substrates using the same precursor HA powder. In the case of the CoBlast technique the resulting HA coating exhibited a relatively homogeneous coverage and a thickness of approximately 2.5 µm. Comparing the MCD and alumina (Al_2O_3) CoBlast abrasives examined, coatings deposited with the latter were found to exhibit increased adhesion, probably associated with increased chemical bonding and mechanical interlocking due to the slightly higher surface area available caused by increased roughening. The close to ambient HA deposition conditions of the CoBlast process were found to eliminate the thermal modification of the HA and alloy surface region that was observed for the APS process. A significant feature of the much thinner CoBlast deposited HA coatings was the absence of cracking within the coating as compared with the APS deposited HA and this may explain the significantly enhanced adhesion observed for the former coatings in tensile tests. The reduction in coating cracking combined with the

retention of the original HA crystallinity should lead to lower dissolution rates of the coating *in vivo*. A further issue with respect to the APS deposited coatings was retention of significant levels of Al_2O_3 within the coating arising from the pre-treatment process used to enhance surface roughness prior to APS processing. This study demonstrates that the CoBlast technique exhibits potential for the deposition of HA onto medical implants, without affecting either the HA crystallinity or substrate mechanical properties, while maintaining equivalent or better cell response as the APS deposited HA coating. Therefore it can be concluded, this ambient temperature process offers a greater opportunity to produce HA surfaces for osteoblast cell proliferation on small, thermally sensitive devices and this may result in enhanced responses *in vivo*.

Acknowledgements

This work is supported by Science Foundation Ireland Grant 08/SRCI1411.

References

[1] L.L. Hench, J. Wilson, An introduction to bioceramics, World Scientific Pub Co Inc, 1993.

[2] S.R. Paital, N.B. Dahotre, Mat Sci Eng R, 66 (2009) 1-70.

[3] L.C. Lucas, W.R. Lacefield, J.L. Ong, R.Y. Whitehead, Colloid Surface A, 77 (1993) 141-147.

[4] H. Wang, N. Eliaz, Z. Xiang, H.P. Hsu, M. Spector, L.W. Hobbs, Biomaterials, 27 (2006) 4192-4203.

[5] L. Sun, C.C. Berndt, K.A. Gross, A. Kucuk, J Biomed Mater Res, 58 (2001) 570-592.

[6] K. de Groot, J.G. Wolke, J.A. Jansen, Proceedings of the Institution of Mechanical Engineers. Part H, Journal of engineering in medicine, 212 (1998) 137-147.

[7] Y.W. Gu, K.A. Khor, P. Cheang, Biomaterials, 24 (2003) 1603-1611.

[8] L. Gan, J. Wang, R.M. Pilliar, Biomaterials, 26 (2005) 189-196.

[9] L.H. Guo, H. Li, Surf Coat Tech, 185 (2004) 268-274.

[10] K. Ozeki, T. Yuhta, Y. Fukui, H. Aoki, Surf Coat Tech, 160 (2002) 54-61.

[11] O. Albayrak, O. El-Atwani, S. Altintas, Surf Coat Tech, 202 (2008) 2482-2487.

[12] C.T. Kwok, P.K. Wong, F.T. Cheng, H.C. Man, Applied Surface Science, 255 (2009) 6736-6744.

[13] J.D. Haman, L.C. Lucas, D. Crawmer, Biomaterials, 16 (1995) 229-237.

[14] R. Gadow, A. Killinger, N. Stiegler, Surf Coat Tech, 205 (2010) 1157-1164.

[15] Y.C. Tsui, C. Doyle, T.W. Clyne, Biomaterials, 19 (1998) 2015-2029.

[16] Y.C. Tsui, C. Doyle, T.W. Clyne, Biomaterials, 19 (1998) 2031-2043.

[17] S.J. Ding, Y.M. Su, C.P. Ju, J.H. Lin, Biomaterials, 22 (2001) 833-845.

[18] F. Fazan, P.M. Marquis, Journal of Materials Science: Materials in Medicine, 11 (2000) 787-792.

[19] W.C. Xue, S.Y. Tao, X.Y. Liu, X.B. Zheng, C.X. Ding, Biomaterials, 25 (2004) 415-421.

[20] R.T.R. McGrann, D.J. Greving, J.R. Shadley, E.F. Rybicki, T.L. Kruecke, B.E. Bodger, Surf Coat Tech, 108 (1998) 59-64.

[21] Y.C. Yang, E. Chang, Biomaterials, 22 (2001) 1827-1836.

[22] Y.C. Yang, E. Chang, Thin Solid Films, 444 (2003) 260-275.

[23] D.J. Forrest, J.C. Shelton, P.J. Gregson, in: Transactions of The Annual Meeting of The Society For Biomaterials in Conjunction With The International Biomaterials Symposium, Toronto, 1996, pp. 324.

[24] S.L. Evans, P.J. Gregson, Materials Letters, 16 (1993) 270-274.

[25] P. Fogarassy, B. Cofino, P. Millet, A. Lodini, IEEE transactions on bio-medical engineering, 52 (2005) 1161-1166.

[26] A.K. Lynn, D.L. DuQuesnay, Biomaterials, 23 (2002) 1937-1946.

[27] T.W. Clyne, S.C. Gill, Journal of Thermal Spray Technology, 5 (1996) 401-418.

[28] R. Pederson, in: Department of Applied physics and Mechnical Engineering Division of Engineering Materials, Lulea University of Technology, 2002, pp. 13.

[29] L. Le Guehennec, A. Soueidan, P. Layrolle, Y. Amouriq, Dental materials : official publication of the Academy of Dental Materials, 23 (2007) 844-854.

[30] B. León, J.A. Jansen, Thin calcium phosphate coatings for medical implants, Springer Verlag, 2008.

[31] A. Boccaccini, S. Keim, R. Ma, Y. Li, I. Zhitomirsky, Journal of The Royal Society Interface, 7 (2010) S581-S613.

[32] C.S. Kim, P. Ducheyne, Biomaterials, 12 (1991) 461-469.

[33] P. Ducheyne, S. Radin, M. Heughebaert, J.C. Heughebaert, Biomaterials, 11 (1990) 244-254.

[34] P. Ducheyne, W. Van Raemdonck, J.C. Heughebaert, M. Heughebaert, Biomaterials, 7 (1986) 97-103.

[35] J.G.S.A.D.C.W. O'Donoghue, D.L.C.C.L. Haverty, in, US-A- 4 950 505; WO-A-03/080140; WO-A-96/16611; WO-A1-02/102431, EP, 2011.

[36] L. O'Neill, C. O'Sullivan, P. O'Hare, L. Sexton, F. Keady, J. O'Donoghue, Surf Coat Tech, 204 (2009) 484-488.

[37] P. O'Hare, B.J. Meenan, G.A. Burke, G. Byrne, D. Dowling, J.A. Hunt, Biomaterials, 31 (2010) 515-522.

[38] L. O'Neill, C. O'Sullivan, P. O'Hare, L. Sexton, F. Keady, J. O'Donoghue, Surface and Coatings Technology, 204 (2009) 484-488.

[39] F. Tan, F. O'Neill, M. Naciri, D. Dowling, M. Al-Rubeai, Acta Biomater, 8 (2012) 1627-1638.

[40] F. Tan, M. Naciri, D. Dowling, M. Al-Rubeai, Biotechnol Adv, 30 (2012) 352-362.

[41] F. Tan, M. Naciri, M. Al-Rubeai, Biotechnol Bioeng, 108 (2011) 454-464.

[42] A. Chebbi, J. Stokes, Journal of Thermal Spray Technology, 21 (2012) 719-730.

[43] V. Jokanovic, B. Jokanovic, D. Izvonar, B. Dacic, Journal of Materials Science: Materials in Medicine, 19 (2008) 1871-1879.

[44] L. Lutterotti, S. Matthies, H.R. Wenk, A.S. Schultz, J.W. Richardson, Journal of Applied Physics, 81 (1997) 594-600.

[45] L. Lutterotti, D. Chateigner, S. Ferrari, J. Ricote, Thin Solid Films, 450 (2004) 34-41.

[46] L. Lutterotti, M. Bortolotti, G. Ischia, I. Lonardelli, H.R. Wenk, Z Kristallogr, 26 (2007) 125-130.

[47] L. Lutterotti, Nucl Instrum Meth B, 268 (2010) 334-340.

[48] J. Wigren, Surface and Coatings Technology, 34 (1988) 101-108.

[49] L.M. Sun, C.C. Berndt, C.P. Grey, Mat Sci Eng a-Struct, 360 (2003) 70-84.

[50] J.A. Clemens, J.G. Wolke, C.P. Klein, K. de Groot, J Biomed Mater Res, 48 (1999) 741-748.

[51] R.B. Heimann, Surface and Coatings Technology, 201 (2006) 2012-2019.

[52] J. Weng, Q. Liu, J.G.C. Wolke, D. Zhang, K. DeGroot, Journal of Materials Science Letters, 16 (1997) 335-337.

[53] K.A. Gross, C.C. Berndt, H. Herman, J Biomed Mater Res, 39 (1998) 407-414.

[54] N. York, (1998).

[55] P.S. Prevéy, Journal of Thermal Spray Technology, 9 (2000) 369-376.

[56] L.M. Gammon, R.D. Briggs, J.M. Packard, K.W. Batson, R. Boyer, C.W. Domby, Metallography and Microstructures of Titanium and Its Alloys, in: ASM Handbook, ASM International: Metallography and Microstructures, ASM International, Member/Customer Service Center, Materials Park, OH, 44073-0002, USA, 2004, pp. 899-917.

[57] F.J. Garcia-Sanz, M.B. Mayor, J.L. Arias, J. Pou, B. Leon, M. Perez-Amor, Journal of Materials Science: Materials in Medicine, 8 (1997) 861-865.

[58] M.K. Beyer, H. Clausen-Schaumann, Chem Rev, 105 (2005) 2921-2948.

[59] M. Konopka, R. Turansky, J. Reichert, H. Fuchs, D. Marx, I. Stich, Phys Rev Lett, 100 (2008) 115503.